Critical behavior of the spontaneous magnetization at marginal dimensionality in $LiHoF_4$

J. A. Griffin and M. Huster
Department of Physics, Laboratory for Research on the Structure of Matter, University of Pennsylvania, Philadelphia, Pennsylvania 19104

Robert J. Folweiler
Sanders Corporation, Nashua, New Hampshire
(Received 28 March 1980)

We have measured the critical behavior of the spontaneous magnetization as a function of temperature for $T \leq T_c$ in the three-dimensional, uniaxial, dipolar-coupled ferromagnet $LiHoF_4$ using elastic-laser-light-scattering techniques. In the reduced-temperature range $1.3 \times 10^{-3} \leq t \leq 1.3 \times 10^{-1}$, we find that the logarithmically corrected mean-field power law $M(T)/M(0) = Bt^{1/2}|\ln|t_0/t||^{1/3}$ fits the data with $T_c = 1.5383 \pm 0.0003$ K, $t_0 = 0.483 \pm 0.046$, and $\chi^2 = 1.34$. We have also fitted the data to $M(T)/M(0) = B|t|^{1/2}|\ln|t||^{1/3}[1 + C_1(\ln|\ln|t||/|\ln|t|) + C_2(1/|\ln|t||)]$ in order to obtain explicitly the corrections to the leading singularities. We find in this fit that $T_c = 1.5382 \pm 0.0003$ K, $C_1 = 0.07 \pm 0.3$, $C_2 = 0.287 \pm 0.07$, and $\chi^2 = 1.26$. Fits to a simple power law $M(T)/M(0) = Bt^{\beta}$ yield $T_c = 1.5370 \pm 0.0002$ K, $\beta = 0.355 \pm 0.005$, and $\chi^2 = 17.2$. We also present measurements of the temperature and magnetic-field dependence of the light scattering in $LiHoF_4$, and the magnetic-field and wavelength dependence of the circular birefringence.

I. INTRODUCTION

Critical phenomena in uniaxial, dipolar-coupled ferromagnets have been the topic of considerable interest as a result of the concept of marginal dimensionality, the spatial dimension at which classical phenomena are separated from nonclassical behavior. Although there are many well-studied examples of critical phenomena, there are only a few known cases in which the marginal dimensionality is experimentally accessible. In magnetic cooperative phenomena the tricritical point of a uniaxial antiferromagnet in an external magnetic field and the critical point in a three-dimensional, uniaxial, dipolar-coupled ferromagnet are the only known, accessible examples of this concept.

Although in all real magnetic materials there is some magnetic dipole-dipole interaction between the magnetic ions, the mechanism which is usually responsible for the long-range magnetic order is the exchange or super-exchange interaction. In some Ising ferromagnetic materials, however, it has recently been found that dipolar interactions dominate the exchange forces, and these materials have been utilized to investigate the experimental consequences of marginal dimensionality. One of the materials on which relatively little work has been completed is $LiHoF_4$, which is ferromagnetic below $T_c = 1.53$ K. Although this material is similar to $LiTbF_4$, on which a number of detailed experiments have been completed, there are several differences in the electronic and magnetic structure that warrant investigation. Firstly, the ground state of $LiHoF_4$ is a true Ising doublet, whereas the ground-state doublet in $LiTbF_4$ is split by 1.2 K as a result of the crystal field. Secondly, the previous measurements of the critical behavior of the magnetic susceptibility in $LiHoF_4$ have indicated little quantitative distinction between the simple nonclassical power-law behavior and the logarithmically corrected mean-field-theory power-law characteristic of marginal dimensionality. Thirdly, the upper limit of the critical region as observed by magnetic susceptibility in $LiHoF_4$ was 1.1×10^{-2}, whereas similar measurements in $LiTbF_4$ determined an upper limit of 1×10^{-1} in reduced temperature. Fourthly, the critical temperature of $LiHoF_4$ is in the superfluid ^{4}He regime, which results in a temperature homogeneity which is substantially superior to that near the critical temperature of $LiTbF_4$.

In this paper we present the results of an experimental study of the temperature dependence of the spontaneous magnetization of the Ising, dipolar-coupled ferromagnet $LiHoF_4$. These results were obtained by measurements of the temperature and mag-

netic field dependence of the intensity of light elastically scattered by the uniaxial ferromagnetic domains in the ordered phase. In Sec. II we present a summary of the concept of marginal dimensionality and a summary of the magnetic and optical properties of $LiHoF_4$. In Sec. III we present a detailed analysis of our results and in Sec. IV we present a discussion of previous work and our conclusions.

II. THEORY

A. Marginal dimensionality in Ising dipolar ferromagnets

The concept of marginal dimensionality and its relation to critical phenomena have been discussed previously, and in this section we will briefly summarize the results that are relevant to Ising, dipolar-coupled ferromagnets.[1–4] The marginal dimensionality d^* is the spatial dimension which separates mean-field theory, classical critical behavior from nonclassical behavior. At spatial dimensions $d > d^*$ simple power-law behavior occurs with mean-field critical-point exponents. At $d < d^*$ simple power-law behavior occurs with nonclassical critical-point exponents, and ϵ, $1/n$, or series expansions may be used to calculate the numerical values of these exponents. However, the convergence properties of such expansions are not well characterized. At $d = d^*$ the renormalization-group equations can be solved without ϵ or $1/n$ expansions and the resultant critical phenomena are described by mean-field power laws that are modified by logarithmic factors.

The numerical value of d^* is determined by the specific details of the system, such as anisotropy and type and range of coupling. A method of determining d^*, apart from the renormalization-group equations, is the Ginzburg criterion, which provides a technique for estimating the importance of fluctuations in the order parameter $\langle(\delta M)^2\rangle$ compared to the value of the order parameter $\langle M^2\rangle$ in the neighborhood of the phase transition.[5] This criterion involves the correlation volume, which is ξ^d in an isotropic exchange-coupled system and ξ^{d+1} in an Ising, dipolar-coupled system, where d is the spatial dimension and ξ is the correlation length. These arguments lead to $d^* = 4$ in the isotropic short-range case and $d^* = 3$ in the Ising, dipolar-coupled one. The explicit behavior of the spontaneous magnetization $M(T)$ at $d = d^*$ has been calculated using renormalization-group techniques, and is given by[2–4]

$$\frac{M(T)}{M(T=0)} = B|t|^{1/2}|\ln|t||^{1/3} \times\left[1 + C_1\left(\frac{\ln|\ln|t||}{\ln|t|}\right) + C_2\left(\frac{1}{\ln|t|}\right)\right] \quad (1)$$

or by

$$\frac{M(T)}{M(T=0)} = B|t|^{1/2}|\ln|t/t_0||^{1/3} , \quad (2)$$

where $(1 + \cdots)$ is now approximately incorporated into the natural logarithm as t_0. The behavior at $d < d^*$ is given by

$$M(T)/M(T=0) = B|t|^{\beta} \quad (3)$$

where B is the amplitude, $t = (T_c - T)/T_c$ is the reduced temperature, and β is the critical-point exponent.

B. Optical properties of $LiHoF_4$

The optical properties of $LiHoF_4$ have been investigated by several techniques. The crystal structure of $LiHoF_4$ is the same as the mineral scheelite $CaWO_4$ with a space group $C_{4h}^6 - I4_1/a$ and a body-centered tetragonal unit cell having $a = 5.20$ Å and $c = 10.90$ Å. There are four Ho^{3+} ions per unit cell each having site symmetry S_4 with the local fourfold axis parallel to (001). The density is 5.72 g/cm^3, there are four formula units per unit cell, and the crystal is optically uniaxial.[6]

The crystal-field splittings and optical properties of the Ho^{3+} ion in $LiHoF_4$ have been investigated by Christenson[7] and in $LiY_{0.98}Ho_{0.02}F_4$ by Karayianis *et al.*[8] The atomic configuration of Ho^{3+} is $4f^{10}$ which has a Hund's rule ground term of $^5I_8$ that is followed by $^5I_7$, $^5I_6$, $^5I_5$, $^5I_4$, $^5F_5$, $^5F_4$, $^5S_2$, etc., in increasing energy. The $4f^9 5d$ atomic configuration starts at approximately 90 000 cm^{-1}. The $^5I_8$ ground term is split into five levels of Γ_1 symmetry, four levels of Γ_2 symmetry, and four levels of Γ_3 and Γ_4 symmetry. The ground state is a Kramer's doublet of Γ_3 and Γ_4 symmetry, the first excited state is a Γ_2 singlet at 8 cm^{-1} = 10.3 K, and the remaining levels are considerably higher in energy. There are optical transitions throughout the near-infrared and visible spectrum, as a result of the $^5I_8$ to $^5I_7$, . . . , transitions and strong-parity-allowed transitions from the $4f^{10}$ to the $4f^9 5d$ starting at 90 000 cm^{-1}.

The magneto-optical features of $LiHoF_4$ have been investigated by Griffin *et al.*[9] and by Battison *et al.*[10] Figures 1 and 2 depict the specific Faraday rotation versus external magnetic field for $1.5 < T < 77$ K and $\lambda = 514.5$ nm and the wavelength dependence of the Verdet constant, respectively. The Faraday rotation in a material of thickness d at a wavelength λ in a magnetic field H is given by

$$\theta = VdH , \quad (4a)$$

where θ is the Faraday rotation and V is the Verdet constant. The specific Faraday rotation is defined by

$$\Phi = \theta/d = \pi(n_{RCP} - n_{LCP})/\lambda , \quad (4b)$$

where n_{RCP} and n_{LCP} are in the indices of refraction for right circularly polarized and left circularly polarized light, respectively. The circular birefringence $n_{RCP}-n_{LCP}$ is given by the equation[11]

$$n_{RCP}-n_{LCP}=K_1\sum_g \rho_g \sum_f (|\langle g|V_{RCP}|f\rangle|^2-|\langle g|V_{LCP}|f\rangle|^2)\left(\frac{\omega^2}{\omega_{gf}^2-\omega^2}\right), \tag{5}$$

where $\sum_f$ is a sum over final optical states, $\sum_g$ is a sum over the ground Γ_3 and Γ_4 states, ρ_g is the occupation probability of the ground states, and $V_{RCP}(V_{LCP})$ is the electric dipole operator for right circularly polarized (left circularly polarized) light, $\hbar\omega_{gf}$ is the energy difference between the ground states $|g\rangle$ and the excited states $|f\rangle$, $\hbar\omega$ is the energy of the incident radiation, and K_1 is a constant. In the case of widely separated levels $|f\rangle$ and $|g\rangle$ this expression can be expanded to yield

$$n_{RCP}-n_{LCP}=K_2\sum_g \rho_g\left(\frac{\omega^2}{\omega_0^2-\omega^2}\right)\sum_f (|\langle g|V_{RCP}|f\rangle|^2-|\langle g|V_{LCP}|f\rangle|^2) \tag{6}$$

which is the "paramagnetic" contribution to the Faraday rotation. Equation (6), as a result of the factor $\sum_g \rho_g$, indicates that the circular birefringence is proportional to the difference in occupation numbers between the Γ_3 and Γ_4 ground-state doublet that splits in the ferromagnetic phase. The temperature dependence illustrated in Fig. 1 also results from this factor. Equation (6) also yields the wavelength dependence of the Faraday rotation illustrated in Fig. 2, as a result of the frequency-dependent factor $\omega^2/(\omega_0^2-\omega^2)$.

In addition to illustrating the above features, Figs. 1 and 2 illustrate the large magnitude of the circular birefringence in $LiHoF_4$. This circular birefringence is also responsible for the elastic light scattering in the ordered phase.[12,13] The ordered magnetic phase in $LiHoF_4$ consists of Ising ferromagnetic domains aligned parallel or antiparallel to the tetragonal c axis. In each domain the occupation-number difference between the Γ_3 and Γ_4 levels, which are split by the ferromagnetic order, produces a large circular birefringence. In the "up" domains that are parallel to the c axis $n_{RCP} >> n_{LCP}$, in the "down" domains that are antiparallel to the c axis $n_{LCP} >> n_{RCP}$; in zero external magnetic field $|n_{RCP}-n_{LCP}|_{up}=|n_{LCP}-n_{RCP}|_{down}$. An electromagnetic wave propagating parallel to the c axis encounters a transmission diffraction grating in which the periodicity is determined by the domain diameter and the phase modulation is determined by the circular birefringence $|n_{RCP}-n_{LCP}|$. At constant $T < T_c$, an external magnetic field applied parallel to the easy axis modifies the ratio of parallel to antiparallel domains in that the parallel domains grow in volume as the antiparallel domains shrink. At the ferromagnetic-to-paramagnetic phase boundary there are only parallel domains, the crystal is optically homogeneous, and elastic scattering ceases. In zero magnetic field, as the tem-

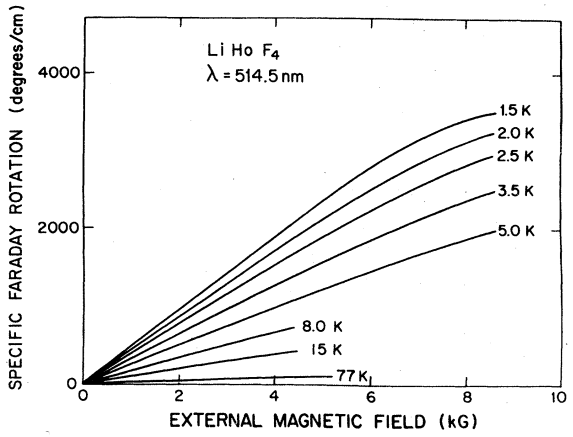

FIG. 1. Specific Faraday rotation vs external magnetic field at $\lambda = 514.5$ nm in $LiHoF_4$ at several temperatures.

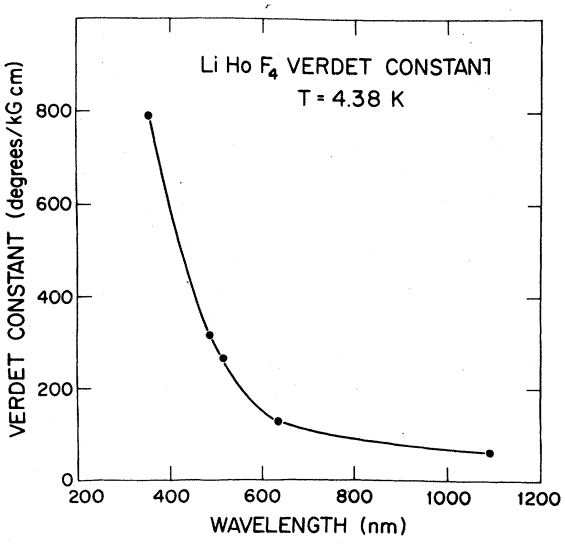

FIG. 2. Verdet constant vs wavelength at $T = 4.38$ K in $LiHoF_4$.

perature is increased, the circular birefringence within a domain is decreased by the thermal disorder until it is zero at and above T_c and again the light scattering ceases. Figures 3 and 4 illustrate the dramatic interaction between the magnetic order and the optical properties of $LiHoF_4$. Figure 3 illustrates the zero-field intensity of scattered light as a function of temperature. The scattered intensity at $T = 1.25$ K is $\sim 100\%$, at $T = 1.45$ K is 94%, at $T = 1.50$ K is 85%, and only in the last 4 mK does the scattering intensity drop precipitously to zero. Figure 4 illustrates the magnetic field dependence of the scattered intensity at $T = 1.515$ K. The intensity of scattered light which is $\sim 75\%$ at zero field drops to zero at a field of 2875 G. This elastic scattering can, therefore, be used as a sensitive probe of the ferromagnetic-paramagnetic coexistence curve by locating $H_c(T)$, the critical external magnetic field on the coexistence curve, as a function of temperature in the H_{ext} vs T plane. Examples of this are depicted in Figs. 5 and 6. Figure 5 illustrates the scattering intensity in a constant-temperature, magnetic field scan. The phase boundary at $T = 1.5148 \pm 0.0002$ K is located at $H_c = 2870 \pm 10$ G. Figure 6 illustrates a constant magnetic field, temperature scan. The phase boundary at $H_c = 3207$ G occurs at $T = 1.5060 \pm 0.0006$ K.

C. Magnetic properties of $LiHoF_4$

The magnetic properties and critical behavior of $LiHoF_4$ have been discussed by Cooke *et al.*[14] and Beauvillain *et al.*,[15] respectively. $LiHoF_4$ orders ferromagnetically at $T_c = 1.53$ K. The Ising behavior results from the Kramer's degeneracy of the Γ_3 and Γ_4 ground-state levels which then form an effective $S = \frac{1}{2}$ for which the tetragonal C axis is the easy axis of magnetization. The g factors have been measured to be $g_{\parallel} = 13.95 \pm 0.15$ and $g_{\perp} = 0.0$ and the Curie-

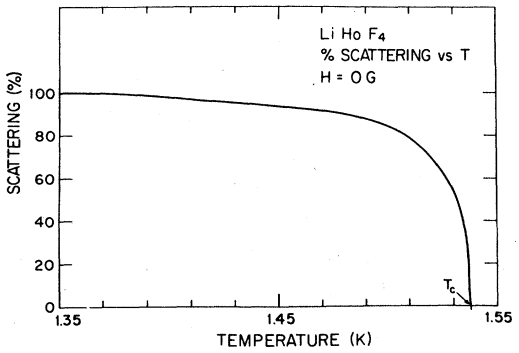

FIG. 3. Zero-field scattering intensity versus temperature in $LiHoF_4$.

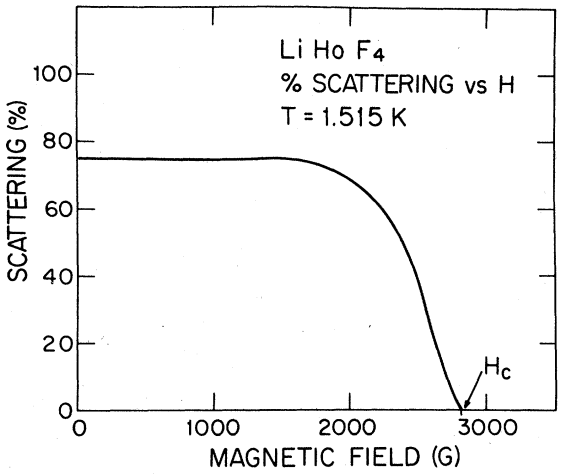

FIG. 4. Scattering intensity vs magnetic field at $T = 1.515$ K in $LiHoF_4$.

Weiss temperature has been measured between 2.5 and 4.0 K to be $\Theta = +0.002 \pm 0.04$ K. Beauvillain *et al.* used this value of Θ in order to determine that the ratio of total exchange to dipolar interaction is $-(11.1 \pm 0.4)/33.46 = -0.332$.[15] Cooke *et al.* have measured a saturation magnetic moment of 892 ± 5

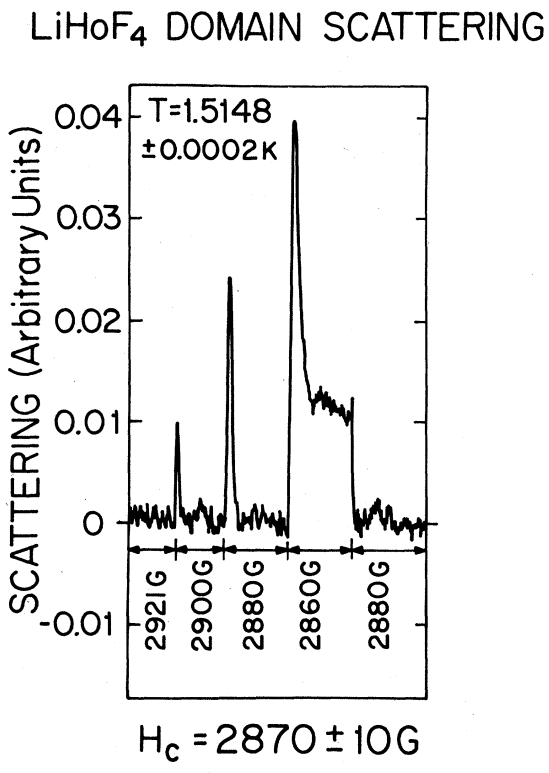

FIG. 5. Scattering intensity near the ferromagnetic-paramagnetic coexistence curve at $T = 1.5148$ K and $H_c = 2870$ G (constant-temperature scan).

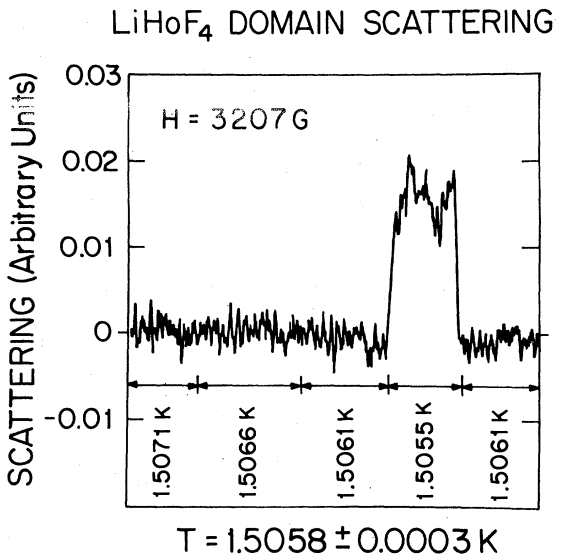

FIG. 6. Scattering intensity near the ferromagnetic-paramagnetic coexistence curve at $H_c = 3207$ G and $T = 1.5060 \pm 0.0006$ K (constant-field scan).

emu/cm^3.[14] The critical behavior of $LiHoF_4$ has been investigated by Beauvillain *et al.* using ac magnetic susceptibility.[15] The observed magnetic susceptibility was compared to both a simple power law $\chi_M = \Gamma|t|^{-\gamma}$ and to the logarithmically modified mean-field-theory behavior $\chi_M = \Gamma|t|^{-1}|\ln|t||^{1/3}$ in the temperature range $3\times10^{-4} < t < 1.1\times10^{-2}$. The power law yielded $\Gamma = (6.2 \pm 0.09)\times10^{-2}$, $T_c = 1.5270$ K, $\gamma = 1.05 \pm 0.01$, and $\chi^2 = 0.64$, whereas using the logarithmic form resulted in $\Gamma = (4.2 \pm 0.07)\times10^{-2}$, $T_c = 1.5299$ K, $t_0 = 7 \pm 3$, and $\chi^2 = 0.70$. Although both forms were found to be adequate fits to the data, it was not possible to eliminate either form based on the magnetic susceptibility. Unlike $LiTbF_4$, measurements of critical behavior of the other thermodynamic functions in $LiHoF_4$ have not yet been completed.

III. EXPERIMENTAL RESULTS AND ANALYSIS

A. Crystal preparation and experimental techniques

The crystal used in this experiment was grown by the Czochralski top-seeded solution technique at Sanders Corporation. It measured $1.3\times1.2\times0.46$ cm^3 with the C axis parallel to the 0.46-cm thickness.

The experimental apparatus utilized in this work is similar to that described by Griffin and Litster,[12] with the exception of the optical cryostat and the method of temperature control. Because $LiHoF_4$ orders at a temperature at which liquid ^{4}He is superfluid, the optical cryostat used in this experiment was constructed such that the sample was immersed in the superfluid helium. This direct immersion improves the thermal homogeneity of the crystal. Temperature control of the cryogenic fluid was obtained by a combination of a manostat, which typically resulted in ±0.5-mK stability, and electronic feedback from an ac resistance bridge. The resistance sensor in this bridge was a 100-Ω carbon resistor wrapped in superconducting lead foil that was located in the liquid ^{4}He but outside the region of the magnetic field in order to avoid magnetoresistance. The sample was mounted on an OFHC copper mount to which an independent, calibrated germanium resistance thermometer was attached. During a typical field scan the temperature stability was ±0.2 mK.

B. Experimental results

Table I enumerates and Fig. 7 illustrates the results of the onset of light scattering in $LiHoF_4$ between 1.338 and 1.537 K. As was discussed in Sec. II B, these data represent the location of the ferromagnetic-paramagnetic phase boundary in the H_{ext} vs T plane. There are 24 points between $10^{-3} < t < 10^{-2}$, 40 points between $10^{-2} < t < 10^{-1}$, and 5 points between $10^{-1} < t < 1.3\times10^{-1}$. In the last two millidegrees below T_c, $H_c(T)$ drops precipitously to zero as the circular birefringence in each domain vanishes. The points for $T < 1.523$ K were taken by isothermal magnetic field scans, and in the range $1.523 < T < 1.537$ K some of the points were taken by scanning temperature while keeping the field constant. In this range the points from the two types of scans were consistent, and no hysteresis was detected. At most points $H_c(T)$ could be determined to $\pm0.5\%$.

In order to analyze the data $H_c(T)$ vs T in Table I, we utilize the fact that in a ferromagnet below T_c the critical magnetic field $H_c(T)$ on the ferromagnetic-paramagnetic phase boundary is related to the spontaneous magnetization $M(T)$ by the equations

$$H_c(T) = NM(T) \tag{7}$$

and

$$M(T)/M(T=0) = H_c(T)/H_c(T=0) \ . \tag{8}$$

In this crystal we could not reach a sufficiently low temperature to extrapolate to the $T=0$ value of H_c, nor could we accurately determine the demagnetization factor. Thus we were unable to determine the amplitude, B. However, we could still fit Eqs. (1)–(3) directly by defining $H_0 = H_c(T=0)B$.

The data in Table I have been quantitatively compared to Eqs. (2) and (3) in order to ascertain the influence of marginal dimensionality, and the results of the nonlinear least-squares fits are summarized in

TABLE I. Phase-boundary magnetic field (proportional to the spontaneous magnetization) and temperature data pairs. The uncertainties in temperature have been converted to equivalent uncertainties in magnetic field.

T (K)	H_c (G)	ΔH_c (G)	T (K)	H_c (G)	ΔH_c (G)
1.3385	6050	15	1.5163	2783	13
1.3464	5987	16	1.5164	2784	16
1.3542	5921	21	1.5182	2718	12
1.3676	5820	11	1.5183	2685	9
1.3787	5708	11	1.5200	2564	19
1.3911	5576	11	1.5202	2585	12
1.3971	5476	11	1.5216	2464	17
1.4027	5422	16	1.5216	2495	7
1.4054	5376	11	1.5217	2511	14
1.4137	5265	11	1.5230	2404	11
1.4204	5171	11	1.5244	2327	10
1.4228	5132	11	1.5251	2251	9
1.4301	5039	11	1.5260	2179	9
1.4386	4916	11	1.5272	2082	9
1.4449	4804	11	1.5274	2041	20
1.4546	4620	12	1.5278	2029	21
1.4615	4501	12	1.5286	1973	13
1.4652	4416	12	1.5291	1932	21
1.4682	4369	10	1.5297	1880	14
1.4727	4242	12	1.5304	1838	20
1.4765	4175	11	1.5310	1754	16
1.4797	4058	13	1.5310	1748	14
1.4910	3743	11	1.5319	1646	14
1.4980	3540	8	1.5326	1564	16
1.4990	3489	10	1.5330	1531	27
1.5016	3423	8	1.5332	1502	24
1.5071	3198	10	1.5337	1431	28
1.5084	3157	10	1.5340	1421	24
1.5095	3101	10	1.5348	1268	31
1.5109	3041	13	1.5350	1237	31
1.5122	2977	10	1.5355	1166	22
1.5126	2965	10	1.5360	1033	34
1.5143	2852	23	1.5362	1021	35
1.5148	2875	13	1.5363	997	18
1.5158	2818	12			

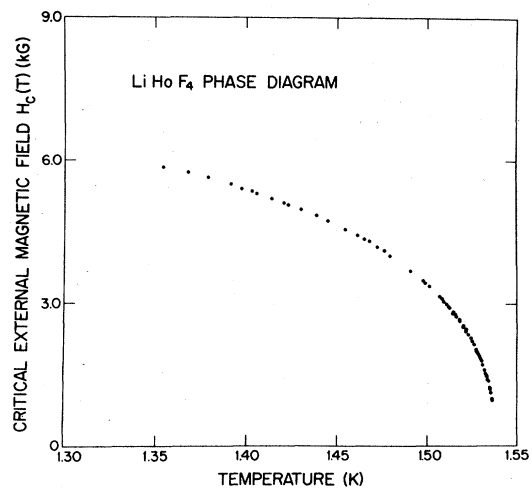

FIG. 7. Phase diagram of $LiHoF_4$. The spontaneous magnetization phase diagram is obtained by the relation $M(T)/M(T=0)=H_c(T)/H_c(T=0)$.

Table II and the best fits are plotted in Figs. 8 and 9. The comparisons between the two possible forms were made over several different ranges in reduced temperature. In the full range given by $1.3\times10^{-3} < t < 1.3\times10^{-1}$ the logarithmic power law fits the data with $\chi^2=1.34$, whereas the nonclassical power law fits the data with $\chi^2=17.2$ with the same number of adjustable parameters in the fit. In this range we obtain $T_c=1.5383\pm0.0003$ K, $H_0=15\,300\pm230$ G, and $t_0=0.48\pm0.05$ using the logarithmically corrected Eq. (2). This value of t_0 is not far from $t_0=0.568\pm0.014$ obtained in $LiTbF_4$ by Griffin and Litster.[12] In this same range we obtain $T_c=1.5370\pm0.0002$ K, $H_0=12\,880\pm180$ G, and $\beta=0.355\pm0.005$, using the simple power-law equation (3). Figures 8 and 9 illustrate the results of these least-squares fits as a function of reduced temperature.

TABLE II. Parameters and equations (see text) utilized to fit data in Table I.

	T	t	H_0 (G)	T_c (K)			χ^2
Logarithmic mean-field with corrections Eq. (1)	$1.338 \leqslant T \leqslant 1.537$	$1.3 \times 10^{-1} \geqslant t \geqslant 1.3 \times 10^{-3}$	15860 ± 250	1.5382 ± 0.0003		$C_1 = 0.068 \pm 0.35$ $C_2 = 0.287 \pm 0.07$	1.26
Logarithmic mean-field Eq. (2)	$1.338 \leqslant T \leqslant 1.537$	$1.3 \times 10^{-1} \geqslant t \geqslant 1.3 \times 10^{-3}$	15300 ± 230	1.5383 ± 0.0003	t_0	0.483 ± 0.046	1.34
	$1.42 \leqslant T \leqslant 1.537$	$7.7 \times 10^{-2} \geqslant t \geqslant 1.3 \times 10^{-3}$	15430 ± 300	1.5382 ± 0.0003		0.456 ± 0.080	1.15
	$1.479 \leqslant T \leqslant 1.537$	$3.8 \times 10^{-2} \geqslant t \geqslant 1.3 \times 10^{-3}$	15530 ± 600	1.5382 ± 0.0004		0.426 ± 0.22	1.12
Power-law Eq. (3)	$1.338 \leqslant T \leqslant 1.537$	$1.3 \times 10^{-1} \geqslant t \geqslant 5 \times 10^{-4}$	12880 ± 180	1.5370 ± 0.0002	β	0.355 ± 0.005	17.2
	$1.42 \leqslant T \leqslant 1.537$	$7.6 \times 10^{-2} \geqslant t \geqslant 6 \times 10^{-4}$	13600 ± 250	1.5373 ± 0.0003		0.370 ± 0.006	7.0
	$1.479 \leqslant T \leqslant 1.537$	$3.8 \times 10^{-2} \geqslant t \geqslant 9 \times 10^{-4}$	14735 ± 900	1.5377 ± 0.0005		0.390 ± 0.010	2.1

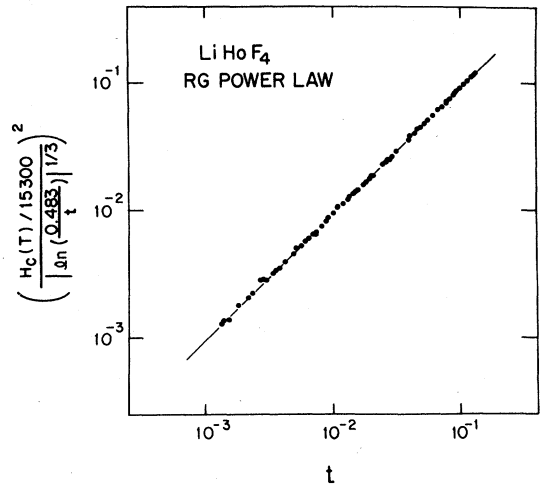

FIG. 8. Best least-squares fit of the logarithmically corrected mean-field power law, Eq. (2).

Figures 10 and 11 dramatically illustrate the difference between these two fits. In these figures the error, the difference between the data and the best fit, is plotted versus reduced temperature. Figure 10 indicates that there is a distribution of error evenly distributed between $\sim \pm 30$ G between $10^{-3} < t < 10^{-1}$ in the fit to equation (2), whereas Fig. 11 indicates that there is a systematic error as a function of temperature in this temperature range in the fit to Eq. (3). Table II also lists the results over other ranges

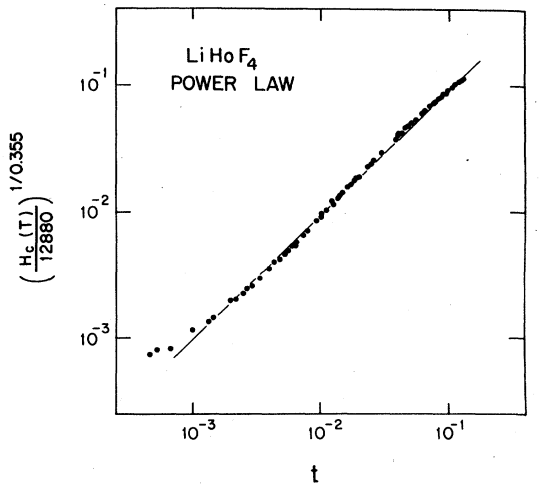

FIG. 9. Best least-squares fit of a nonclassical power law, Eq. (3).

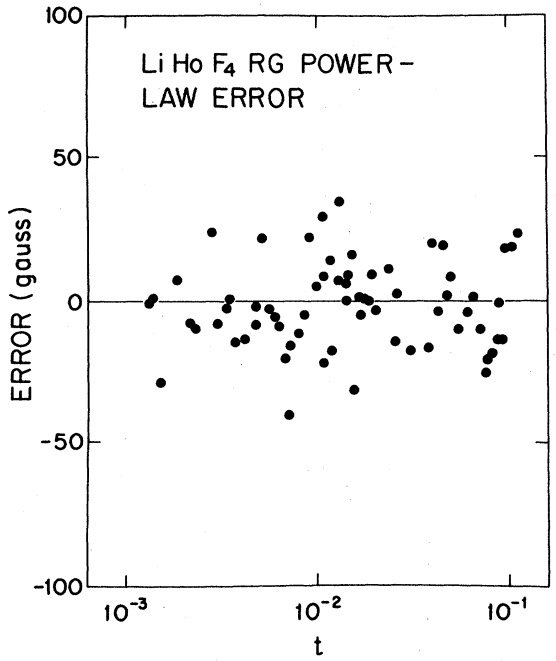

FIG. 10. Plot of the error, the difference between the best fit and the data in Fig. 8, as a function of reduced temperature.

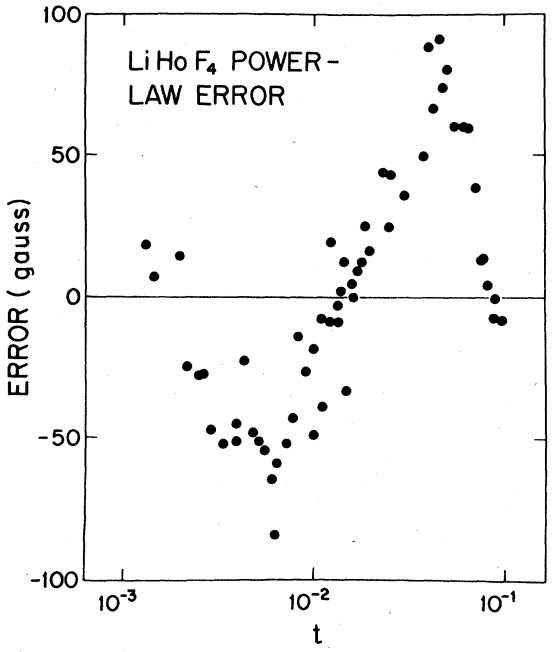

FIG. 11. Plot of the error, the difference between the best fit and the data in Fig. 9, as a function of reduced temperature.

in reduced temperature. Table II indicates that $1.12 < \chi^2 < 1.34$ for fits of Eq. (2) and that $2.1 < \chi^2 < 17.2$ for fits of Eq. (3). The logarithmically corrected power law, therefore, not only fits the observed behavior with a substantially smaller χ^2 than the nonclassical power law, but it also results in a fit that is relatively insensitive to the range of reduced temperature selected for the fit. Moreover, the parameters obtained in the fits of the logarithmic forms are relatively insensitive to the range in fit, whereas the opposite is true in the fits to the nonclassical power law.

The above analysis clearly demonstrates that Eq. (2) presents an accurate representation of the spontaneous magnetization in the critical region of $LiHoF_4$. Equation (2), however, contains the parameter t_0 that is used to represent the collective effect of the higher-order correction terms in Eq. (1). Brezin and Zinn-Justin have calculated C_1 for the susceptibility and specific heat above T_c,[4] but neither C_1 nor C_2 has been calculated for the magnetization below T_c. We have fitted our results to Eq. (1) in order to obtain explicitly numerical values for C_1 and C_2, and the results of this fit are also listed in Table II. We obtain $C_1 = 0.07 \pm 0.30$ and $C_2 = 0.29 \pm 0.07$ in the range $1.3 \times 10^{-3} < t < 1.3 \times 10^{-1}$ with $\chi^2 = 1.2$. It is interesting to note that we have determined that C_1 is very small and poorly determined, but that C_2 is large and accounts for most of the contribution to t_0. These results represent the first experimental determination of the logarithmic corrections to the leading logarithmic singularities at marginal dimensionality.

IV. DISCUSSION

The concept of marginal dimensionality and its effect on critical phenomena have received considerable theoretical and experimental interest, and there have been numerous experimental studies of the consequences of this effect. In most cases, however, it has been difficult to differentiate quantitatively between the predicted logarithmically corrected mean-field behavior and simple nonclassical power-law behavior. Beauvillain *et al.*, using magnetic susceptibility in the range $2 \times 10^{-4} < t < 1.1 \times 10^{-2}$, found $\chi^2 = 0.70$ for the logarithmic form and $\chi^2 = 0.65$ for the nonclassical power law in $LiTbF_4$ (Ref. 16) and in the range $3 \times 10^{-4} < t < 1.1 \times 10^{-1}$, $\chi^2 = 0.70$ for the logarithmic form and $\chi^2 = 0.64$ for the nonclassical power law in $LiHoF_4$.[15] Ahlers *et al.* measured the specific heat in $LiTbF_4$ above and below T_c, but agreement with logarithmic behavior was found only over one decade in reduced temperature.[17] Als-Nielsen *et al.*, using neutron scattering, have measured the temperature dependence of the magnetic susceptibility,[18] the spontaneous magnetization,[19] and the correlation length[20]

in $LiTbF_4$. In measurements of the susceptibility and magnetization they were not able to detect logarithmic factors, but in measurements of the correlation length, when coupled with the specific-heat data of Ahlers *et al.*, they were able to obtain agreement with two nontrivial universal amplitude relationships predicted by renormalization-group theory. They could not, however, see logarithmic corrections to the correlation range. Frowein *et al.*,[21] using a superconducting quantum interference device (SQUID) magnetometer, carefully measured the equation of state in $LiTbF_4$ near T_c. They found that for an Ising, dipolar equation of state $\chi^2 = 1.1$, for a short-range, Ising equation of state $\chi^2 = 2.5$, and for a mean-field equation of state $\chi^2 = 4.8$.

In the experiment described in this paper we have obtained the temperature dependence of the spontaneous magnetization in the neighborhood of the critical point in $LiHoF_4$ using elastic light scattering from the ferromagnetic domains. In the reduced-temperature range $1.3 \times 10^{-3} < t < 1.3 \times 10^{-1}$ we have fitted our data to a nonclassical power law with an exponent $\beta = 0.355 \pm 0.005$ and a resultant $\chi^2 = 17.2$. Over the same reduced-temperature range we have fitted our data to a logarithmically corrected mean-field power law with $\chi^2 = 1.34$ and $t_0 = 0.483 \pm 0.046$. Moreover, we have quantitatively determined the amplitudes C_1 and C_2 that occur in the correction to the leading singularity to be $C_1 = 0.07 \pm 0.3$ and $C_2 = 0.29 \pm 0.07$. We believe that this experiment represents one of the most conclusive, quantitative verifications of the existence of marginal dimensionality.

ACKNOWLEDGMENTS

We wish to thank J. J. Folkins for the fitting programs, discussions about the data analysis, and assistance in taking the Faraday rotation data. This work was supported by the National Science Foundation under Grant No. DMR 77-23409, by the National Science Foundation MRL Grant No. DMR 76-80994, and by the Research Corporation.

[1]K. G. Wilson and J. Kogut, Phys. Rev. C 12, 75 (1974); M. E. Fisher, Rev. Mod. Phys. 46, 597 (1974); S. K. Ma, *ibid.* 45, 589 (1973); S. K. Ma, *Modern Theory of Critical Phenomena* (Benjamin, New York, 1976); P. Pfeuty and G. Toulouse, *Introduction to the Renormalization Group and to Critical Phenomena* (Wiley, New York, 1979).

[2]A. I. Larkin and D. E. Khmel'nitskii, Zh. Eksp. Teor. Fiz. 56, 2087 (1969) [Sov. Phys. JETP 29, 1123 (1969)]; A. Aharony, Phys. Rev. B 8, 3342, 3349, 3358, 3363 (1973); F. J. Wegner and E. H. Riedel, *ibid.* 7, 248 (1973).

[3]A. Aharony and B. I. Halperin, Phys. Rev. Lett. 35, 1308 (1975).

[4]E. Brezin and J. Zinn-Justin, Phys. Rev. B 13, 251 (1976).

[5]V. L. Ginsberg, Fiz. Tverd. Tela 2, 2031 (1960) [Sov. Phys. Solid State 2, 1824 (1960)]; J. Als-Nielsen and R. J. Birgeneau, Am. J. Phys. 45, 554 (1977).

[6]C. Keller and H. Schmutz, J. Inorg. Nucl. Chem. 27, 900 (1965); R. E. Thoma, C. D. Brunton, R. A. Penneman, and T. K. Keenan, Inorg. Chem. 9, 1096 (1970).

[7]H. P. Christensen, Phys. Rev. B 19, 6564 (1979).

[8]N. Karayianis, D. E. Wortman, H. P. Jenssen, J. Phys. Chem. Solids 37, 675 (1976).

[9]J. A. Griffin, J. Folkins, M. Huster, D. Gabbe, and I. Laursen (unpublished).

[10]J. E. Battison, A. Kasten, M. J. M. Leask, J. B. Lowry, and B. M. Wanklyn, J. Phys. C 8, 4089 (1975).

[11]M. J. Weber, R. Morgret, S. Y. Leung, J. A. Griffin, D. Gabbe, and A. Linz, J. Appl. Phys. 49, 3464 (1978); W. A. Crossley, R. W. Cooper, J. L. Page, and R. P. Van Stapele, Phys. Rev. 181, 896 (1969).

[12]J. A. Griffin and J. D. Litster, Phys. Rev. B 19, 3676 (1979); J. A. Griffin, J. D. Litster, and A. Linz, Phys. Rev. Lett. 38, 251 (1977).

[13]J. F. Dillon, Jr., E. Yi Chen, H. J. Guggenheim, and Richard Alben, Phys. Rev. B 15, 1422 (1977); J. A. Griffin, S. E. Schnatterly, Y. Farge, M. Regis, and M. P. Fontana, *ibid.* 10, 1960 (1974); J. F. Dillon, Jr., and J. P. Remeika, J. Appl. Phys. 34, 637 (1963); J. C. Suits, *ibid.* 38, 1498 (1967).

[14]A. H. Cooke, D. A. Jones, J. F. A. Silva, and M. R. Wells, J. Phys. C 8, 4083 (1975).

[15]P. Beauvillain, J. P. Renard, I. Laursen, and P. J. Walker, Phys. Rev. B 18, 3360 (1978); P. Beauvillain, Ph.D. thesis (Université de Paris, Orsay, 1979) (unpublished).

[16]P. Beauvillain, C. Chappert, and I. Laursen (unpublished).

[17]G. Ahlers, A. Kornblit, and H. J. Guggenheim, Phys. Rev. Lett. 34, 1227 (1975).

[18]J. Als-Nielsen, L. M. Holmes, and H. J. Guggenheim, Phys. Rev. Lett. 32, 610 (1974).

[19]J. Als-Nielsen, L. M. Holmes, F. Krebs Larsen, and H. J. Guggenheim, Phys. Rev. B 12, 191 (1975).

[20]J. Als-Nielsen, Phys. Rev. Lett. 37, 1161 (1976).

[21]R. Frowein, J. Kötzler, and W. Assmus, Phys. Rev. Lett. 42, 739 (1979).